HHS Public Access

Author manuscript

Exp Eye Res. Author manuscript; available in PMC 2017 December 01.

Published in final edited form as:

Exp Eye Res. 2014 December ; 129: 18–23. doi:10.1016/j.exer.2014.10.005.

A Comparative Analysis of C57BL/6J and 6N Substrains; Chemokine/Cytokine Expression and Susceptibility to Laser-Induced Choroidal Neovascularization

Gloriane Schnabolk[1], **Kimberly Stauffer**[2], **Elizabeth O'Quinn**[2], **Beth Coughlin**[2], **Kannan Kunchithapautham**[2], and **Bärbel Rohrer**[1,2,*]

[1]Research Service, Ralph H Johnson VA Medical Center, Charleston, SC 29401

[2]Department of Ophthalmology, Medical University of South Carolina, Charleston, SC 29425

[3]Department of Neurosciences, Medical University of South Carolina, Charleston, SC 29425

Abstract

Age-related macular degeneration (AMD) is the most prevalent cause of blindness in the elderly. To study potential underlying mechanisms of AMD, animal models are utilized, focusing mostly on mice. Recently, genomic and phenotypic differences between the so-called control substrains, C57BL/6J and C57BL/6N, have been described in models of ocular and non-ocular diseases. In particular, the rd8 mutation of the *Crb1* gene present in the C57BL/6N has been shown to impact certain ocular phenotypes and appears to augment phenotypes generally associated with inflammation. Here, we investigated angiogenic factor and cytokine expression using pathway arrays as well as the susceptibility to laser-induced choroidal neovascularization (CNV), a model of wet AMD, in the two substrains. Age-matched 3-month-old C57BL/6J and C57BL/6N animals differed in gene expression levels for angiogenic factors and cytokines, with 6N animals expressing higher levels of inflammatory markers than 6Js. Yet laser-induced CNV was comparable in size between the two substrains. This lack of difference in CNV size was correlated with a gene expression profile that was comparable between the two substrains, due to the fact that the degree of change in gene expression of inflammatory markers after CNV was blunted in 6N mice. In summary, significant gene expression differences exist between C57BL/6J and C57BL/6N animals, reinforcing the notion that appropriate litter-mate controls or genetic background controls need to be used. Contrary to our expectation, CNV was not augmented in 6N animals, suggesting that low chronic inflammation in the RPE might provide a level of pre-conditioning and protection against stress.

[*]**Corresponding author**: Department of Ophthalmology, Medical University of South Carolina, 167 Ashley Avenue, Charleston, SC 29425; phone: (843) 792-5086; fax (843) 792-1723; rohrer@musc.edu.

Keywords

rd8 mutation; choroidal neovascularization; age-related macular degeneration; para-inflammation; pre-conditioning

The most commonly used animal species to study models of age-related macular degeneration (AMD) is the mouse. Models include structural perturbations through laser photocoagulation (Rohrer et al., 2009) or subretinal PEG-8 injections (Lyzogubov et al., 2011) as well as a large number of genetically-altered animals (Pennesi et al., 2012). For all these models, genetically-homogenous inbred mice are used to reduce variability within experiments, improve reproducibility of experiments between different laboratories, and enable genetic mapping of effects of variance in strains. However, mutations and consequent genetic drift do occur. The original inbred C57BL/6J mouse strain was established at the Jackson Laboratory from the parental strain C57BL in 1948. In 1951, the F32 generation was moved to the National Institutes of Health, which resulted in the development of the C57BL/6N line. This genetic separation of the two substrains C57BL/6J and C57BL/6N by ~220 generations (Mekada et al., 2009) resulted in the presence of a couple of thousand single nucleotide polymorphisms (SNPs)(Yalcin et al., 2012), producing 34 SNPs and 2 indels in coding sequences that differ between the two strains, in addition to 15 structural variants that overlap a gene (Simon et al., 2013). These genetic variations are associated with changes in phenotypes, including ocular phenotypes (Luhmann et al., 2012), differences in rates of obesity (Heiker et al., 2014), susceptibility to cocaine (Kumar et al., 2013), and most likely others. Finally, despite the fact that AMD is an aging disease, the typical age group for CNV studies for pharmacology and pathway analyses is ~3 months of age. At that age, the eye has reached its final adult size and shape, which allows for consistent placement of the CNV lesions.

Two of the main differences between the two strains are in the *Nnt* and the *Crb1* genes (Mekada et al., 2009). The *Nnt* gene encodes the nicotinamide nucleotide transhydrogenase protein, located on the inner mitochondrial membrane. This enzyme is responsible for reducing NADP+ and NAD+ to NADPH and NADH. In doing this, it helps regulate cellular redox homeostasis, apoptotic events, and energy use (Yin et al., 2012). A naturally occurring mutation arose in the C57BL/6J line between 1976 and 1984, in which exons 7-11 of *Nnt* were deleted. This deletion causes the NNT protein to be absent; this mutation has been associated with impaired glucose homeostasis control and reduced insulin secretion. In addition, NADPH acts as a cofactor to glutathione reductase, which regenerates the antioxidant glutathione. Without this pathway to regenerate the antioxidant, oxidative stress might be higher in these animals. The RD8 mutation on the other hand is in the *Crb1* gene, encoding for a protein that is important for external limiting membrane integrity and photoreceptor development. This is an autosomal recessive, single nucleotide deletion that gives rise to a retinal degeneration phenotype (Mattapallil et al., 2012); and *Crb* variants in humans have been demonstrated in retinal diseases such as retinitis pigmentosa and Leber congenital amaurosis (Mehalow et al., 2003), and may contribute to AMD pathogenesis.

AMD occurs in two forms: wet and dry. Dry AMD leads to the slow degeneration and atrophy of the photoreceptors in the macula by mechanisms not fully understood; wet AMD is associated with choroidal neovascularization (CNV) in the area of the macula and leakage of these new vessels. AMD has age as a risk factor; however, other environmental and epidemiologic factors appear to play a role in the disease process. In particular smoking, light damage, body mass index, and race have been reported to be associated with disease risk (Chakravarthy et al., 2010). It is now accepted that an overactive complement system is tied to the incidence of AMD, based on histological, biochemical and genetic data (Zipfel et al., 2010). Other inflammatory or angiogenic factors that contribute to AMD include the pro-angiogenic factor vascular endothelial growth factor (VEGF), hepatocyte growth factor/scatter factor (HGF/SF), platelet-derived growth factor (PDGF), acidic and basic fibroblast growth factor (aFGF and bFGF) as well as tumor necrosis factor-α (TNF-α) and the anti-angiogenic factor pigment epithelium-derived factor (PEDF) (de Oliveira Dias et al., 2011; Tatar et al., 2006). In addition, inflammatory cytokines such as interleukin (IL)-1β and IL-18 (Campbell and Doyle, 2013), IL-17 (Liu et al., 2011), chemokines such as CCL2 and CX3CL1 (Raoul et al., 2010), and others may contribute to disease progression. Despite this inflammatory profile, patients with AMD do exhibit overt ocular inflammation, but rather demonstrate sterile inflammation in the diseased eyes (Whitcup et al., 2013).

Here we wished to identify the significance of genotypic differences of the two C57BL/6 substrains, 6J and 6N at 3-months-of age as they pertain to CNV and sterile inflammation.

For these studies, all experiments were performed in accordance with the ARVO Statement for the Use of Animals in Ophthalmic and Vision Research and were approved by the University Animal Care and Use Committee. Female and male mice from the two substrains, C57BL/6J (Jackson Laboratories, Indianapolis, IN) and C57BL/6N (Taconic, Hudson, NY) were utilized. Each mouse was genotyped prior to the study to confirm the presence and/or absence of the *Nnt* or *Crb1* variant, using primers designed to distinguish between the *Nnt* (Nicholson et al., 2010) or *Crb1* (Mattapallil et al., 2012) variants. Genotyping confirmed that the C57BL/6J mice have the *Nnt* exon 7-11 deletion, but are wild type for the rd8 locus; whereas the C57BL/6N mice are wild type for the *Nnt* and mutant for the rd8 locus (**Fig. 1A**).

A priori, based on the presence or absence of the *Nnt* and the *Crb1* genes, differences in cellular homeostasis are predicted. Without the *Nnt* gene, the gene product which helps regulate cellular redox homeostasis, apoptotic events, and energy use, tissues might experience higher levels of oxidative stress. Likewise, the rd8 variant might exacerbate conditions of inflammation and contribute to AMD pathogenesis (Luhmann et al., 2012; Mattapallil et al., 2012; Tuo et al., 2004). To determine the effects of the two genotypes on their chemokine/cytokine profiles, the Mouse Inflammatory Response and Autoimmunity RT^2 Profiler PCR array (Cat # PAMM-077Z; SABiosciences, Frederick, MD) were utilized according to the manufacturer's instructions. RPE-choroid fractions were isolated from control and CNV eyes 6 days following laser-induced photocoagulation of Bruch's membrane. Tissues from 4-6 animals were pooled for each strain from each experimental condition, RNA extracted and cDNA generated for hybridization. Fold change in gene expression was calculated using the web-based module provided by the array manufacturer.

Results were returned as relative gene expression level [2^(−avgΔCt)] with genes of interest normalized to the arithmetic mean of the five housekeeping genes provided, *Actb* (beta actin), *B2m* (beta-2 microglobulin), *Gapdh* (glyceraldehyde-3-3phosphate dehydrogenase), *Gus* (glucoronidase, beta) and *Hsp90ab1* (heat shock protein 90 alpha, class B member 1). The arithmetic mean of the house keeping genes among the four groups and six comparisons did not differ significantly (ANOVA; treatment effect: $P=0.28$; with individual P-values ranging from 0.09-0.87). At 3-months-of-age, the C56BL/6N substrain with the rd8 mutation was found to have higher expression levels of chemokines and cytokines when compared to the 6J animals (**Table IA**). Of the 80 genes present on the array, 35 of the genes were differentially expressed ($P<0.05$ and ≥2-fold change), 28 of which can be classified as pro-inflammatory, 7 of which are anti-inflammatory or contribute to homeostasis. On average, the pro-inflammatory genes were increased in expression (5.63 ±1.59; Z test, $P<0.001$), whereas the anti-inflammatory and homeostasic components were no different from zero (1.93 ±3.92; Z test, $P=0.3$) indicative of an inflammatory phenotype. Increased expression is noted in particular for complement component 3 (*C3*), the complement component 3a receptor 1 (*C3ar1*), the chemokine (C-C motif) receptor 2 (*Ccr2*) and interleukin 17A (*Il-17a*), gene products thought to be associated with AMD.

Since the 6N mice appear to have an inflammatory phenotype when compared to the 6J strain, it was of interest whether the 6N strain would exhibit greater susceptibility to CNV development. CNV lesions were induced in four spots per eye surrounding the optic nerve as described by us previously, using argon-laser photocoagulation (532 nm, 100 μm spot size, 0.1 s duration, 100 mW) (Rohrer et al., 2009). CNV lesions were assessed using optical coherence tomography (OCT) on day 5 after laser-photocoagulation of Bruch's membrane (**Fig. 1B**) using a SD-OCT Bioptigen® Spectral Domain Ophthalmic Imaging System (Bioptigen Inc., Durham, NC). Rectangular volume scans set at 1.6 × 1.6 mm, consisting of 100 B-scans (1000 A-scans per B-scan) were performed. Cross-sectional area of the lesions was determined using methods described by Giani et al. in which and the en-face fundus reconstruction tool was used to determine the center of the lesion by identifying the midline passing through the area of the RPEBruch's membrane rupture with the axial interval positioned at the level of the RPE/choroid complex (Giani et al., 2011). Using vertical calipers at the site of each lesion, the area of the hyporeflective spot produced in the fundus image was calculated with the aid of ImageJ software (National Institutes of Health, Bethesda, MD). The mean CNV lesion area was determined by averaging lesion spot sizes from each eye for 6J and 6N animals, indicating that the two genotypes were equally susceptible to CNV (**Fig. 1C**) (CNV size measured in pixel density; 6J: 3,323 ±203; 6N: 3,322 ±212; t test, $P=1.0$).

The lack of greater susceptibility to a chemokine/cytokine-dependent disease process in the 6N mice suggests that the constant exposure of the ocular tissues to a pro-inflammatory condition, presumably from birth, might precondition the eye to be less prone to inflammation. PCR arrays were compared within each genotype as well as between the two genotypes for changes in gene expression in response to CNV. Of the 80 genes present on the array, 19 of the genes were differentially expressed in the RPE-choroid samples from 6N mice (16/3 pro- versus anti-inflammatory) (**Table IB**); 31 genes were altered in the 6J

samples (26/5 pro- versus anti-inflammatory) (**Table IC**) (P <0.05 and ≥2-fold change). In the 6N samples, the differences were centered on a median of -2.62 (-19.7 to 5.5) when including all genes, or -2.77 (-6.8 to 5.5) when excluding the anti-inflammatory or homeostatic genes, which in both cases, did not differ from zero (Z test, P =0.98). In the 6J samples, the Z test indicated a pro-inflammatory state when analyzing all genes together (median of 2.53; range of -3.8 to 19.8; Z test, P <0.002), or when excluding the anti-inflammatory or homeostatic genes (median of 3.01; range of -3.8 to 19.8; Z test, P <0.0004). Of the genes that were differentially expressed in the two genotypes, 11 were found to overlap, (pro-inflammatory genes: *Ccl12*, *Ccl2*, *Ccl5*, *Ccl7*, *Ccr3*, *Cxcl10*, *Cxcl5*, *Il1a* and *Il1rn*; and anti-inflammatory or homeostatic genes: *Cebpd* and *Il23a*); and of those pro-inflammatory genes, with the exception of *Il1a*, *Il1rn* which were upregulated in both substrains, all the cytokines/chemokine genes were elevated in the 6J strain in CNV when compared to the 6J control and downregulated in the 6N strain in CNV when compared to its substrain control. Finally, the comparison of the gene expression response to CNV between the two genotypes revealed that only 8 genes were found to differ (**Table 1D**) (median of -2.59; range of -4.7 to 5.1), with all 8 genes belonging to the pro-inflammatory category. Overall, the inflammatory state of the two substrains induced by CNV was comparable (Z test, P <0.8). The main results of the current study are: 1) Genetic profiling for cytokines and chemokines indicated an elevated pro-inflammatory state in the unperturbed 6N mouse retina which are wild type for the *Nnt* gene but carry a mutation for the rd8 locus when compared to those isolated from C57BL/6J mice which carry a mutation in the *Nnt* gene, but are wild type for the rd8 locus. 2) Laser-induced CNV was, however, comparable in size between the 6J and 6N mice. 3) CNV resulted in a large increase in expression of inflammatory markers in 6J mice, whereas this response was significant blunted in 6N mice. 4) Interestingly, however, when comparing the gene expression differences between 6J and 6N strain in the presence of CNV, the differences were minor. This reduction in apparent inflammation in 6N mice during the disease state together with comparable CNV development between the two substrains, suggests that compensatory mechanisms reminiscent of pre-conditioning against stress such as para-inflammation, might be present in the 6N eyes; however further experiments, beyond the scope of this report, are required to support this hypothesis

The experiments described here were designed to determine whether the *Crb1* variant plays a role in choroidal neovascularization and inflammation. Based on the known role for the *Crb1* gene product in external limiting membrane integrity and photoreceptor development, the observed confounding effects of the rd8 variant on the phenotype of the *Ccl2/Cx3cr1*$^{-/-}$ mice (Luhmann et al., 2013), and the protective role for anti-inflammatory tumor necrosis factor-inducible-gene 6 (TSG-6) in the rd8-positive *Ccl2/Cx3cr1*$^{-/-}$ mice, augmentation of CNV was predicted in the 6N mice. The Mouse Inflammatory Response and Autoimmunity RT^2 Profiler PCR arrays confirmed an inflammatory phenotype in the 6N substrain retinas when compared to the 6J animals at baseline (**Table IA**). Despite this elevated levels of angiogenic factors and pro-inflammatory cytokines in the 6N retinas prior to laser photocoagulation, CNV lesion sizes were comparable between the two substrains (**Figure 1B**). In addition, the inflammatory response triggered by the CNV lesions was significantly suppressed in the 6N animals (**Table IB**), resulting in gene expression changes in response

to CNV that were statistically indistinguishable between the two substrains (**Table 1D**). It is unclear whether the inflammatory response in the 6J mouse retina is entirely due to the CNV lesions or whether the lack of *Nnt* might also contribute to the observed response. It has been noted by Ronchi and coworker (Ronchi et al., 2013) that *Nnt* loss of function results in mitochondrial redox abnormalities, leading to a reduction in NADP and glutathione in their reduced states. Since CNV results in increased oxidative stress [e.g., (Dong et al., 2009)], a loss of reducing agents might augment the inflammatory response exhibited by the 6J mice. On the flip side, the reduced inflammatory response in the 6N mice in response to CNV might represent a compensatory mechanism akin to pre-conditioning. Similar to our results obtained in the eye demonstrating a larger inflammatory response in the RPE-choroid from 6J mice, Simon and colleagues reported that 6J mice showed enhanced dinitrofluorobenzene-induced contact hypersensitivity when compared to 6N mice, that was correlated with a greater responsiveness of natural killer cells to IL-12 or IL-12/IL-2 co-stimulation (Simon et al., 2013).

An elevated level of low-grade inflammation in the presence of an up-regulation of anti-inflammatory molecules might represent “para-inflammation”, a term fist coined by Medzhitov to describe an inflammatory response in between healthy homeostasis and chronic inflammation (Medzhitov, 2008). This mechanism appears to allow adaptation of cells and tissues to a stressful environment while maintaining adequate functionality. However, if the stressor is not removed, para-inflammation gives way chronic inflammation, and pathology may develop (Whitcup et al., 2013; Xu et al., 2009). In the 6N animals in the absence of a stressor, the changes in gene expression in RPE-choroid when compared to those in the 6J mice represent a mix of pro- and anti-inflammatory cytokines and homeostatic and inflammatory chemokines (**Table IA**). Observed elevated mRNA of anti-inflammatory or homeostatic genes included *Il-10* and *Ccl19*; and elevated pro-inflammatory molecules included *Il-18*, *Il-1a*, *Ccl11*, *Cxcl4*, *Ccl5*, *Ccl8* and *Ccr3*. It will be of great interest to further explore the protective and damaging effects of para-inflammation in the context of AMD models and human disease. Likewise, it would be of great interest to explore the effect of aging on cytokine and chemokine expression in these strains. In addition, differences in susceptibility to treatment should be explored. Do the altered levels of cytokines and chemokines present in the different substrains change the mice's response profile to treatments such as anti-VEGF or compounds that target the complement system? Or in other words, could different baseline levels of cytokines and chemokines prior to disease determine whether a patient is a responder or non-responder using particular treatment regiments – a question the field of pharmacogenetics explores (Schwartz and Brantley, 2011). We will attempt to answer some of these questions in future studies.

While it has been appreciated that mouse strain-related phenotypic differences exist, such as those differences between DBA/1, Swiss, C57BL/6, and BALB/c, SV129 and others, only recently have substrain-related phenotypic differences such as those between C57BL/6J and 6N been reported (Heiker et al., 2014; Kumar et al., 2013; Luhmann et al., 2012). A recent analysis using Next-Generation sequencing, identified a total of 56.7 million single nucleotide polymorphism (SNP) sites between the 17 mouse strain analyzed. As expected, the number of SNPs varied based on genetic distance between the strains, being the smallest

(couple of thousand) for the C57BL/6J versus 6N comparison (Yalcin et al., 2012). Similarly, the NCBI SNP database (dbSNP Build 141) lists ~72.4 million SNPs for humans. And according to the International Society of Genetic Genealogy (ISOGG), the number of shared SNPs varies between 73-74.6% for unrelated people of European descent; or in other words, two unrelated people differ by 18.4-19.6 million SNPs. However, the number of SNPs that have phenotypic consequence are still unknown. From a patient perspective, these SNP numbers together with our data on substrain-specific gene-expression differences reinforce the importance of recognizing inter-patient genetic variability both when designing and when choosing medications for a particular patient and disease. From a research perspective, it is important to keep in mind the potential relationship between the genomic variants and phenotypes examined. This is particularly important if knockout or transgenic mice are used. While for many SNPs there may be little or no phenotype effect, pathology might be caused by combining the effects of SNPs with altering genes by genetic manipulations (e.g., (Luhmann et al., 2013) or by interactions between SNPs and the environment. Finally, it needs to be recognized that a single mouse strain might be more representative of a single individual, and hence to more closely examine human responses many different mouse strains might have to be examined, a strategy typically not feasible in research.

Acknowledgements

We thank Luanna Bartholomew for critical review. This work was supported in the laboratory of B.R. in part by the National Institutes of Health (NIH R01EY019320), a Department for Veteran Affairs merit award RX000444, the Beckman Initiative for Macular Research, an unrestricted grant to MUSC from Research to Prevent Blindness (RPB), New York, NY, Foundation Fighting Blindness, Columbia, MD, and a summer undergraduate stipend from Wofford College to K.S. (John Rampey Fund). Animal studies were conducted in a facility constructed with support from the NIH C06RR015455.

REFERENCES

Campbell M, Doyle SL. An eye on the future of inflammasomes and drug development in AMD. Journal of molecular medicine. 2013; 91:1059–1070. [PubMed: 23661041]

Chakravarthy U, Wong TY, Fletcher A, Piault E, Evans C, Zlateva G, Buggage R, Pleil A, Mitchell P. Clinical risk factors for age-related macular degeneration: a systematic review and meta-analysis. BMC ophthalmology. 2010; 10:31. [PubMed: 21144031]

de Oliveira Dias JR, Rodrigues EB, Maia M, Magalhaes O Jr. Penha FM, Farah ME. Cytokines in neovascular age-related macular degeneration: fundamentals of targeted combination therapy. Br J Ophthalmol. 2011; 95:1631–1637. [PubMed: 21546514]

Dong A, Xie B, Shen J, Yoshida T, Yokoi K, Hackett SF, Campochiaro PA. Oxidative stress promotes ocular neovascularization. J Cell Physiol. 2009

Giani A, Thanos A, Roh MI, Connolly E, Trichonas G, Kim I, Gragoudas E, Vavvas D, Miller JW. In vivo evaluation of laser-induced choroidal neovascularization using spectral-domain optical coherence tomography. Invest Ophthalmol Vis Sci. 2011; 52:3880–3887. [PubMed: 21296820]

Heiker JT, Kunath A, Kosacka J, Flehmig G, Knigge A, Kern M, Stumvoll M, Kovacs P, Bluher M, Kloting N. Identification of genetic loci associated with different responses to high fat diet induced obesity (DIO) in C57BL/6N and C57BL/6J substrains. Physiol Genomics. 2014

Kumar V, Kim K, Joseph C, Kourrich S, Yoo SH, Huang HC, Vitaterna MH, de Villena FP, Churchill G, Bonci A, et al. C57BL/6N mutation in cytoplasmic FMRP interacting protein 2 regulates cocaine response. Science. 2013; 342:1508–1512. [PubMed: 24357318]

Liu B, Wei L, Meyerle C, Tuo J, Sen HN, Li Z, Chakrabarty S, Agron E, Chan CC, Klein ML, et al. Complement component C5a promotes expression of IL-22 and IL-17 from human T cells and its implication in age-related macular degeneration. J Transl Med. 2011; 9:1–12.

Luhmann UF, Carvalho LS, Robbie SJ, Cowing JA, Duran Y, Munro PM, Bainbridge JW, Ali RR. Ccl2, Cx3cr1 and Ccl2/Cx3cr1 chemokine deficiencies are not sufficient to cause age-related retinal degeneration. Exp Eye Res. 2013; 107:80–87. [PubMed: 23232206]

Luhmann UF, Lange CA, Robbie S, Munro PM, Cowing JA, Armer HE, Luong V, Carvalho LS, MacLaren RE, Fitzke FW, et al. Differential modulation of retinal degeneration by Ccl2 and Cx3cr1 chemokine signalling. PLoS One. 2012; 7:e35551. [PubMed: 22545116]

Lyzogubov VV, Tytarenko RG, Liu J, Bora NS, Bora PS. Polyethylene glycol (PEG)-induced mouse model of choroidal neovascularization. J Biol Chem. 2011; 286:16229–16237. [PubMed: 21454496]

Mattapallil MJ, Wawrousek EF, Chan CC, Zhao H, Roychoudhury J, Ferguson TA, Caspi RR. The Rd8 mutation of the Crb1 gene is present in vendor lines of C57BL/6N mice and embryonic stem cells, and confounds ocular induced mutant phenotypes. Invest Ophthalmol Vis Sci. 2012; 53:2921–2927. [PubMed: 22447858]

Medzhitov R. Origin and physiological roles of inflammation. Nature. 2008; 454:428–435. [PubMed: 18650913]

Mehalow AK, Kameya S, Smith RS, Hawes NL, Denegre JM, Young JA, Bechtold L, Haider NB, Tepass U, Heckenlively JR, et al. CRB1 is essential for external limiting membrane integrity and photoreceptor morphogenesis in the mammalian retina. Hum Mol Genet. 2003; 12:2179–2189. [PubMed: 12915475]

Mekada K, Abe K, Murakami A, Nakamura S, Nakata H, Moriwaki K, Obata Y, Yoshiki A. Genetic differences among C57BL/6 substrains. Exp Anim. 2009; 58:141–149. [PubMed: 19448337]

Nicholson A, Reifsnyder PC, Malcolm RD, Lucas CA, MacGregor GR, Zhang W, Leiter EH. Diet-induced obesity in two C57BL/6 substrains with intact or mutant nicotinamide nucleotide transhydrogenase (Nnt) gene. Obesity (Silver Spring). 2010; 18:1902–1905. [PubMed: 20057372]

Pennesi ME, Neuringer M, Courtney RJ. Animal models of age related macular degeneration. Mol Aspects Med. 2012; 33:487–509. [PubMed: 22705444]

Raoul W, Auvynet C, Camelo S, Guillonneau X, Feumi C, Combadiere C, Sennlaub F. CCL2/CCR2 and CX3CL1/CX3CR1 chemokine axes and their possible involvement in age-related macular degeneration. J Neuroinflammation. 2010; 7:87. [PubMed: 21126357]

Rohrer B, Long Q, Coughlin B, Wilson RB, Huang Y, Qiao F, Tang PH, Kunchithapautham K, Gilkeson GS, Tomlinson S. A targeted inhibitor of the alternative complement pathway reduces angiogenesis in a mouse model of age-related macular degeneration. Invest Ophthalmol Vis Sci. 2009; 50:3056–3064. [PubMed: 19264882]

Ronchi JA, Figueira TR, Ravagnani FG, Oliveira HC, Vercesi AE, Castilho RF. A spontaneous mutation in the nicotinamide nucleotide transhydrogenase gene of C57BL/6J mice results in mitochondrial redox abnormalities. Free Radic Biol Med. 2013; 63:446–456. [PubMed: 23747984]

Schwartz SG, Brantley MA Jr. Pharmacogenetics and age-related macular degeneration. Journal of ophthalmology. 2011; 2011:252549. [PubMed: 22046503]

Simon MM, Greenaway S, White JK, Fuchs H, Gailus-Durner V, Wells S, Sorg T, Wong K, Bedu E, Cartwright EJ, et al. A comparative phenotypic and genomic analysis of C57BL/6J and C57BL/6N mouse strains. Genome Biol. 2013; 14:R82. [PubMed: 23902802]

Tatar O, Adam A, Shinoda K, Stalmans P, Eckardt C, Luke M, Bartz-Schmidt KU, Grisanti S. Expression of VEGF and PEDF in choroidal neovascular membranes following verteporfin photodynamic therapy. Am J Ophthalmol. 2006; 142:95–104. [PubMed: 16815256]

Tuo J, Smith BC, Bojanowski CM, Meleth AD, Gery I, Csaky KG, Chew EY, Chan CC. The involvement of sequence variation and expression of CX3CR1 in the pathogenesis of age-related macular degeneration. Faseb J. 2004; 18:1297–1299. [PubMed: 15208270]

Whitcup SM, Sodhi A, Atkinson JP, Holers VM, Sinha D, Rohrer B, Dick AD. The role of the immune response in age-related macular degeneration. Int J Inflam. 2013; 2013:348092. [PubMed: 23762772]

Xu H, Chen M, Forrester JV. Para-inflammation in the aging retina. Prog Retin Eye Res. 2009; 28:348–368. [PubMed: 19560552]

Yalcin B, Adams DJ, Flint J, Keane TM. Next-generation sequencing of experimental mouse strains. Mamm Genome. 2012; 23:490–498. [PubMed: 22772437]

Yin F, Sancheti H, Cadenas E. Silencing of nicotinamide nucleotide transhydrogenase impairs cellular redox homeostasis and energy metabolism in PC12 cells. Biochim Biophys Acta. 2012; 1817:401–409. [PubMed: 22198343]

Zipfel PF, Lauer N, Skerka C. The role of complement in AMD. Adv Exp Med Biol. 2010; 703:9–24. [PubMed: 20711704]

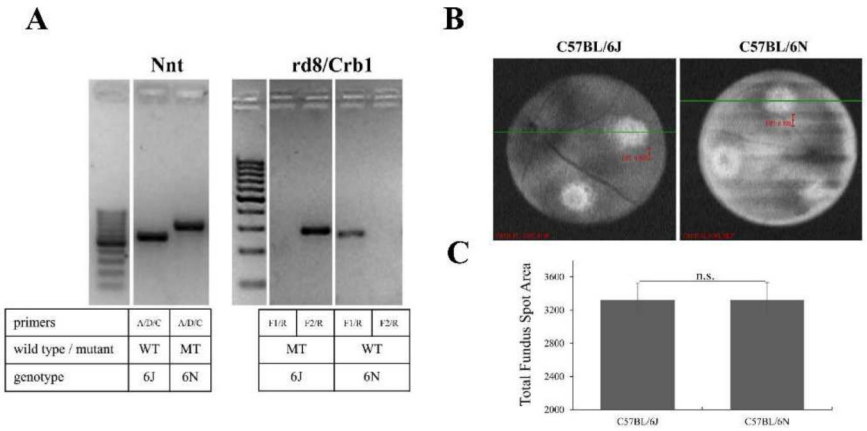

FIGURE 1. CNV development in C57BL/6J and 6N mice

(A) PCR genotyping of C57BL/6J and 6N strains. Tail DNA was used in separate PCR reactions, using primers designed to distinguish between the *Nnt* (NntA-COM, NntD-WT and NntC-MUT; abbreviated in Figure as A, D and C respectively) or *Crb1* (mF1, mF2 and mR; abbreviated in Figure as F1, F2 and R respectively) variants. NntA-COM and NntD-WT amplify the *Nnt* wild type (579 bp), NntA-COM and NntC-MUT the *Nnt* mutant gene (743 bp); mF1 and mR amplify the *Crb1* wild type (220 bp), and mF2 and mR the mutant allele (244 bp). Amplified DNA samples were run with an aliquot of a 100 bp ladder for molecular weight detection. Due to the similarity in amplicon size for the *Crb1* wild type and knockout allele, the wild type and mutant primer set reactions were carried out separately for each DNA template; and to compensate for the larger mF2 primer, the primer amounts for the smaller two primers mF1 and mR were doubled in the amplification reactions. Hence the 6J stain is *Nnt* mutant, and *Crb1* wild type; the 6N strain is *Nnt* wild type, and *Crb1* mutant.

CNV development was assessed in C57BL/6J and 6N mice. CNV lesions were induced in cohorts of age-matched C57BL/6J and C57BL/6N mice using laser photocoagulation. (**B**) The size of the lesions was assessed using optical coherence tomography (OCT) and representative images are presented. (**C**) CNV size was quantified by image analyses and presented as numbers of pixels. No strain-specific differences were observed. Data are expressed as mean ±SEM (n =12-14 animals per genotype).

TABLE I

Cytokine and chemokine mRNA levels in RPE-choroid fractions in C57BL/6J and 6N mice, comparing gene expression at baseline and after CNV induction.

Gene Name	Gene Symbol	Sequence	Fold Change	*P*-value	Role
(A) ***6N Control versus 6J Control***					
B-cell leukemia/lymphoma 6	Bcl6	NM_009744	2.0811	0.001516	I
Chemokine (C-C motif) ligand 22	Ccl22	NM_009137	−3.4806	0.006794	I
Chemokine (C-C motif) receptor 3	Ccr3	NM_009914	−6.7085	0.000207	I
Chemokine (C-X-C motif) ligand 2	Cxcl2	NM_009140	−8.6099	0.003704	I
Chemokine (C-X-C motif) ligand 9	Cxcr9	NM_008599	−3.0937	0.012427	I
Interleukin 10	Il10	NM_010548	2.0056	0.001654	A
Interleukin 10 receptor, beta	Il10rb	NM_008349	−9.5533	0.00001	A
Interleukin 22	Il22	NM_016971	−4.6139	0.000252	A
Complement component 3	C3	NM_009778	8.6378	0.001789	I
Complement component 3a receptor 1	C3ar1	NM_009779	4.6611	0.000014	I
Chemokine (C-C motif) ligand 11	Ccl11	NM_011330	13.7117	0.001924	I
Chemokine (C-C motif) ligand 19	Ccl19	NM_011888	23.2206	0.01528	H
Chemokine (C-C motif) ligand 24	Ccl24	NM_019577	3.1763	0.000893	I
Chemokine (C-C motif) ligand 25	Ccl25	NM_009138	−2.3016	0.004093	I
Chemokine (C-C motif) ligand 4	Ccl4	NM_013652	7.314	0.004979	I
Chemokine (C-C motif) ligand 5	Ccl5	NM_013653	16.4955	0.000701	I
Chemokine (C-C motif) ligand 7	Ccl7	NM_013654	8.4405	0.000027	I
Chemokine (C-C motif) ligand 8	Ccl8	NM_021443	2.5562	0.000049	I
Chemokine (C-C motif) receptor 1	Ccr1	NM_009912	4.8928	0.000489	I
Chemokine (C-C motif) receptor 2	Ccr2	NM_009915	13.9675	0.000029	I
Chemokine (C-X-C motif) ligand 1	Cxcl1	NM_008176	30.6398	0.003108	I
Chemokine (C-X-C motif) ligand 3	Cxcl3	NM_203320	24.7725	0.000337	I
Chemokine (C-X-C motif) receptor 2	Cxcr2	NM_009909	2.9026	0.004689	I
Interleukin 17A	Il17A	NM_010552	2.9773	0.000312	I
Interleukin 18	Il18	NM_008360	2.6586	0.000108	I
Interleukin 1 alpha	Il1a	NM_010554	5.148	0.001206	I
Interleukin 1 receptor accessory protein	Il1rap	NM_008364	2.6586	0.043514	A
Interleukin 6	Il6	NM_031168	−2.1475	0.007518	A
Interleukin 9	Il9	NM_008373	3.8388	0.00147	I
Lymphotoxin A	Lta	NM_010735	4.1144	0.000623	I
Nuclear receptor subfamily 3, group C, member 1	Ptgs2	NM_008173	2.1101	0.002178	H
Receptor (TNFRSF)-interacting serine-threonine kinase 2	Sele	NM_138952	3.3496	0.049676	I
Toll-like receptor 2	Tlr2	NM_011905	3.8123	0.010768	I
Toll-like receptor 6	Tlr6	NM_011604	6.122	0.002262	I
Toll-like receptor 7	Tlr7	NM_133211	3.243	0.015145	I
(B) ***6N CNV versus 6N Control***					
Complement component 3	C3	NM_009778	−2.8706	0.000361	I

Gene Name	Gene Symbol	Sequence	Fold Change	*P*-value	Role
Chemokine (C-C motif) ligand 12	Ccl12	NM_011331	−6.8274	0.000413	I
Chemokine (C-C motif) ligand 2	Ccl2	NM_011333	−6.5644	0.000063	I
Chemokine (C-C motif) ligand 5	Ccl5	NM_013653	−2.4646	0.002731	I
Chemokine (C-C motif) ligand 7	Ccl7	NM_013654	−5.2343	0.000078	I
Chemokine (C-C motif) ligand 8	Ccl8	NM_021443	−19.671	0.000015	H
Chemokine (C-C motif) receptor 2	Ccr2	NM_009915	−5.61	0.000017	I
Chemokine (C-C motif) receptor 3	Ccr3	NM_009914	−3.6503	0.00051	I
CCAAT/enhancer binding protein (C/EBP), beta	Cebpb	NM_009883	2.0638	0.02968	A
Chemokine (C-X-C motif) ligand 10	Cxcl10	NM_021274	−2.2995	0.000203	I
Chemokine (C-X-C motif) ligand 5	Cxcl5	NM_009141	−4.4527	0.000736	I
FBJ osteosarcoma oncogene	Fos	NM_010234	2.1219	0.003137	I
Interleukin 1 alpha	Il1a	NM_010554	2.1715	0.006116	I
Interleukin 1 receptor antagonist	Il1rn	NM_031167	3.3839	0.00005	I
Interleukin 23, alpha subunit p19	Il23a	NM_031252	2.1715	0.020853	H
Selectin, endothelial cell	Sele	NM_011345	−2.7664	0.000515	I
Toll-like receptor 5	Tlr5	NM_016928	2.1465	0.001296	I
Chemokine (C-C motif) ligand 17	Ccl17	NM_011332	5.5481	0.000279	I
Chemokine (C-X-C motif) ligand 1	Cxcl1	NM_008176	−5.6752	0.00362	I
Lymphotoxin B	Ltb	NM_008518	−2.1705	0.048025	I
(C) *6J CNV versus 6J Control*					
Chemokine (C-C motif) ligand 11	Ccl11	NM_011330	−3.8602	0.000007	I
Chemokine (C-C motif) ligand 12	Ccl12	NM_011331	2.0917	0.026205	I
Chemokine (C-C motif) ligand 2	Ccl2	NM_011333	2.5164	0.010004	I
Chemokine (C-C motif) ligand 24	Ccl24	NM_019577	−3.2013	0.001955	I
Chemokine (C-C motif) ligand 5	Ccl5	NM_013653	2.3262	0.002233	I
Chemokine (C-C motif) ligand 7	Ccl7	NM_013654	2.0018	0.035961	I
Chemokine (C-C motif) receptor 4	Ccr4	NM_009916	−2.6366	0.004484	I
CCAAT/enhancer binding protein (C/EBP), beta	Cebpb	NM_009883	−2.415	0.012722	A
Chemokine (C-X-C motif) ligand 3	Cxcl3	NM_203320	−3.3839	0.00629	I
Interleukin 10 receptor, beta	Il10rb	NM_008349	2.2366	0.000513	A
Interleukin 17A	Il17a	NM_010552	−2.7741	0.003539	I
Interleukin 1 beta	Il1b	NM_008361	4.2713	0.002068	I
Interleukin 23, alpha subunit p19	Il23a	NM_031252	−3.471	0.010454	I/A
Interleukin 5	Il5	NM_010558	2.5339	0.046348	I
Interleukin 6	Il6	NM_031168	−3.6859	0.00479	A
Interleukin 9	Il9	NM_008373	−2.8986	0.001341	I
Myeloid differentiation primary response gene 88	Myd88	NM_010851	3.0133	0.003196	I
Toll-like receptor 7	Tlr7	NM_133211	4.3309	0.00384	I
Complement component 3a receptor 1	C3ar1	NM_009779	4.3711	0.001137	I
Complement component 4B (Childo blood group)	C4b	NM_009780	4.0596	0.0009	I
Chemokine (C-C motif) ligand 25	Ccl25	NM_009138	2.3861	0.00169	I
Chemokine (C-C motif) receptor 3	Ccr3	NM_009914	4.1163	0.000392	I

Gene Name	Gene Symbol	Sequence	Fold Change	*P*-value	Role
Chemokine (C-X-C motif) ligand 10	Cxcl10	NM_021274	9.305	0.000046	I
Chemokine (C-X-C motif) ligand 5	Cxcl5	NM_009141	19.8078	0.000009	I
Chemokine (C-X-C motif) receptor 4	Cxcr4	NM_009911	3.0413	0.001434	I
Interleukin 18	Il18	NM_008360	3.3434	0.000079	H
Interleukin 1 alpha	Il1a	NM_010554	11.1683	0.000004	I
Interleukin 1 receptor antagonist	Il1rn	NM_031167	11.272	0.000056	I
Integrin beta 2	Itgb2	NM_008404	3.1123	0.00046	I
Lymphocyte antigen 96	Ly96	NM_016923	2.2679	0.003222	I
Toll-like receptor 3	Tlr3	NM_126166	3.3745	0.002153	I
Toll-like receptor 5	Tlr5	NM_016928	12.1369	0.000071	I
(D) *6N CNV vs 6J CNV*					
Chemokine (C-C motif) ligand 8	Ccl8	NM_021443	−2.0543	0.000662	I
Chemokine (C-X-C motif) ligand 1	Cxcl1	NM_008176	2.1406	0.0167	I
Chemokine (C-X-C motif) ligand 5	Cxcl5	NM_009141	−3.5603	0.000002	I
Interleukin 17A	Il17a	NM_010552	−3.2686	0.019877	I
Interleukin 9	Il9	NM_008373	−3.1282	0.002106	I
Toll-like receptor 5	Tlr5	NM_016928	−4.6546	0.00004	I
Chemokine (C-C motif) ligand 17	Ccl17	NM_011332	5.103	0.000491	I
Prostaglandin-endoperoxide synthase 2	Ptgs2	NM_011198	2.5515	0.000336	I

cDNA was analyzed in triplicates using the Mouse Inflammatory Response and Autoimmunity RT^2 Profiler PCR array as described in Material and Methods. Differentially expressed genes (P <0.05 and ≥2-fold change) are presented, listing gene symbol, sequence ID, fold change in gene expression and the corresponding P value, as well as their role in inflammation (I – inflammatory, A – antiinflammatory, or H –homeostatic). See text for interpretation of the data. (**A**) 35/80 of the genes were differentially expressed between the two strains at baseline; (**B**) 19/80 of the genes were differentially expressed in C57BL/6N mice between the CNV and control condition; (**C**) 31/80 of the genes were differentially expressed in C57BL/6J mice between the CNV and control condition; and (**D**) 8/80 of the genes were significantly different between the two substrains in response to CNV. For each gene, gene symbol, sequence ID, fold change in gene expression, and the corresponding P value as well as their role in inflammation (I – inflammatory, A – antiinflammatory, or H –homeostatic) are listed. See text for interpretation of the data.